04

Nonlinear oscillations in a Bursian diode with a time-dependent external voltage

© V.I. Kuznetsov, V.Yu. Koyokin, L.A. Bakaleinikov

Ioffe Institute,
St. Petersburg, Russia
e-mail: koiokin@mail.ru

Received September 5, 2025
Revised November 20, 2025
Accepted November 24, 2025

Time-dependent processes developing in a vacuum diode with an electron flow when a sinusoidal perturbation is added to the constant potential difference applied between the electrodes have been studied. It is established that an oscillatory process with a period determined by the frequency of the external perturbation develops in the diode plasma. Three fundamentally different modes of oscillation generation have been found, depending on the amplitude of the external voltage. It is shown that plasma dynamics in these modes is closely related to stationary solutions, which correspond to the collector potential value at various time moments.

Keywords: Bursian diode, time-dependent boundary conditions, nonlinear oscillations.

DOI: 10.61011/TP.2026.03.63159.249-25

Introduction

In the 21st century, the world's interest in thermionic converters (TIC) doesn't fade away. This is mainly caused by a need to generate high power (100 KW and higher) for spacecraft. TIC is traditionally treated as a converter of heat (from a nuclear reactor or solar radiation) into DC electrical power (see [1–4]). However, such diode can also directly generate alternating current. For this, it is sufficient to connect its electrodes through an external inductive element [5]. In this case, energy accumulation on this element and energy discharge into an external circuit occur alternatively in a diode – external circuit system during a transient process. Occurrence of oscillations in TIC is only possible when TIC is used in collisionless mode. This is associated with a potential development of electronic instability in plasma leading to a sudden current interruption [6].

Two problems shall be solved for parameter optimization of such oscillator. Firstly, it shall be identified how an inductive element of an external circuit affects the development of electronic instability, and inductances, at which electronic instability develops, shall be determined. This problem was solved in [7,8], where it is shown that instability can develop only in some inductance domains. Secondly, nonlinear stage of instability development shall be calculated to find the best oscillation mode and determine the optimum converter efficiency. The presence of an inductive element in the external circuit is functionally equivalent to a variable boundary condition on a collector. This study investigates how an alternating external voltage affects the behavior of nonlinear processes in the diode plasma.

As shown in [6], during the oscillatory process in TIC, when both ions and electrons move, electronic instability develops at certain points in time, and considerable potential redistribution in plasma occurs during times approximately equal to the time of electron transit through the inter-electrode gap. Ions can be considered as fixed ones at this oscillation stage, and it is sufficient to examine only electron dynamics. A vacuum electron-beam diode (Bursian diode) is the simplest electronic diode. It also serves as the simplest kinetic model of a plasma gap for investigating the processes taking plase in various high-current plasma electronic devices. For example, in microwave devices such as klystrons, vircators and reflex triodes (see [9,10]). Here, electron beam energy is converted into high-amplitude electric field oscillations followed by electromagnetic radiation generation. New diode modes of operation are proposed to increase conversion efficiency: formation of several virtual cathodes [11], using the external harmonic effect on the virtual cathode modulation depth [12]. Control of complex nonlinear modes in plasma systems with a virtual cathode is also an important problem, in particular, large focus is made on investigating the capabilities of chaos control [13] and intentional state switching in diodes via external periodic disturbances [14].

The aim of this study is to perform theoretical and numerical investigations of nonlinear oscillations and possible transient process flow scenarios in the Bursian diode induced by external sinusoidal disturbance. Analytical theory is built for small disturbance amplitudes. For large amplitudes, characteristics of transient processes in plasma are studied numerically. This included the analysis of scenarios of nonlinear oscillation development in diode plasma.

1. Problem formulation

The study explores the Bursian diode, i.e. a flat diode, where an electron beam arrives from an emitter at a mean velocity $\overline{v}_0 > 0$ and density n_0 and moves without collisions in the interelectrode gap. Let the difference of potentials between the collector and emitter spaced at the distance d be constant and equal to U. In which case distribution of potential $\Phi(z)$ with the electric field strength $E = -\partial_z \Phi$ occurs in the gap. A particle reaching any of the electrodes is assumed to be absorbed at the electrode.

For convenience, we proceed to dimensionless quantities, selecting the electron energy at the emitter $W_0 = m\overline{v}_0^2/2$ and Debye–Hückel length as the units of energy and length. $\lambda_D = \left[2\tilde{\epsilon}_0 W_0/(e^2 n_0)\right]^{1/2}$ (here e, m are the electron charge and -mass, and $\tilde{\epsilon}_0$ is the vacuum permittivity). For dimensionless coordinate, potential, electric field strength, velocity and time, we have: $\xi = z/\lambda_D$, $\eta = e\Phi/(2W_0)$, $\varepsilon = eE\lambda_D/(2W_0)$, $u = v/\overline{v}_0$, $\tau = t/(\lambda_D/\overline{v}_0)$. Electrodes spacing is $\tau = t/(\lambda_D/\overline{v}_0)\delta = d/\lambda_D$, and the difference of potentials is . $V = eU/(2W_0)$.

The following problem will be solved. Assume that before the time $\tau = \tau_0$, where τ_0 constitutes several times of electron transit through the interelectrode gap, the difference of potentials between the electrodes is equal to V_0, and from the time τ_0 the collector potential starts oscillating with the amplitude $|\Delta V|$:

$$V(\tau;\omega) = V_0 + \Delta V \sin[\omega(\tau - \tau_0)]\Theta(\tau - \tau_0). \qquad (1)$$

Here, $\Theta(x)$ is the Heaviside function We analyze potential scenarios of transient process flow induced by the collector potential oscillations $V(\tau)$ (1).

For this purpose, we first explore steady-state solutions for the values of V falling within $(V_0 - \Delta V, V_0 + \Delta V)$. Steady-state solutions for the Bursian diode are characterized by potential distributions (PD) with one minimum, whose value is denoted as η_m. In the case when the initial electron energy is higher than $|\eta_m|$, the electron will reach the collector. Otherwise, it will be reflected from the potential barrier — a virtual cathode (VC), and will return to the emitter. When calculating PD, the electron velocity distribution function at the emitter $f_0(u_0)$ is chosen in the form of an „arch“ with a narrow velocity spread.

$$f_0(u_0) = (2\Delta)^{-1}\Theta\left[\Delta^2 - (1 - u_0)^2\right], \quad \Delta \ll 1. \qquad (2)$$

Stationary solutions were studied by many authors (see, for example, [15,16]). It is convenient to represent them as points in the plane (ε_0, δ), where δ and ε_0 are dimensionless electrode spacing and electric field strength at the emitter. At a fixed value of V , these points form separate curves (solution branches). Figure $1, a$ shows solution branches for a set of external voltages V from the interval $(-0.5, -0.3)$, and Figure $1, b$ shows a dimensionless minimum value at PD η_m. It can be seen that there are three steady-sate solutions within some δ range — three branches: lower (normal), middle (overlap) and upper (a branch with electron reflection from VC).

The right-hand bifurcation point on the solution branch (interface point of the normal and overlap branches) is called the SCL point. A left-hand bifurcation point (interface point of the middle and upper branches) is called the BF point. In [16], it is shown that for a case when $f_0(u_0)$ is the δ-function, coordinates of the SCL point are calculated as follows

$$\delta_{SCL} = \frac{\sqrt{2}}{3}\left(1 + \sqrt{1 + 2V}\right)^{3/2},$$

$$\varepsilon_0^{SCL} = \sqrt{2}\left(1 + \sqrt{1 + 2V}\right)^{-1/2},$$

$$\eta_m^{SCL} = -\frac{1}{2}(1 + 2\sqrt{1 + 2V})(1 + \sqrt{1 + 2V})^{-2}, \qquad (3)$$

and coordinates of the BF point are calculated as follows

$$\delta_{BF} = \frac{\sqrt{2}}{3}\left[1 + (1 + 2V)^{3/4}\right], \quad \varepsilon_0^{BF} = \sqrt{2}. \qquad (4)$$

In the case of slightly smeared $f_0(u_0)$, δ_{SCL} decreases, and δ_{BF} increases by a value on the order of Δ^2 (note that it is true up to V greater than $-1/2$ by several values of Δ), and δ_{BF} increases by a value on the order of $\sqrt{\Delta}$, which is already a relatively high value (for example, at $\Delta = 0.01$ it turns out to be on the order of 0.1).

Thus, it can be seen that a steady-state solution ambiguity region for each value of V is limited by the $(\delta_{BF}(V), \delta_{SCL}(V))$ interval. It has been found that solutions corresponding to the normal branch and solutions from the upper branch for $\delta < \delta_{SCL}$ are stable with respect to small-amplitude disturbances, and solutions corresponding to the overlap branch are instable [16,17]. Steady-state solutions will be widely used for the analysis of transient solutions for a diode with a time-varying collector potential.

2. Various transient process versions

Consider potential scenarios of transient processes in the diode plasma. Let the initial diode state correspond to $\delta = 0.75$, $V = V_0 = -0.40$ and is positioned on the normal branch (Figure $1, a$), i.e. its electric field strength at the emitter ε_0 is the lowest of the three solutions — $\varepsilon_{0,\min}(-0.40, 0.75) = 1.0711$. A point in the (ε_0, δ) plane corresponding to this state is located between the $\delta_{BF}(V)$ and $\delta_{SCL}(V)$ bifurcation points. We slowly change the collector potential, assuming that the oscillation period $T_\omega = 2\pi/\omega$ is much longer than the time of electron transit through the interelectrode gap T.

The transient process will initially flow, changing between the steady-state solutions located on the normal branches. However, further progress of the process will be defined by the collector potential oscillation amplitude ΔV. Three scenarios can be expected.

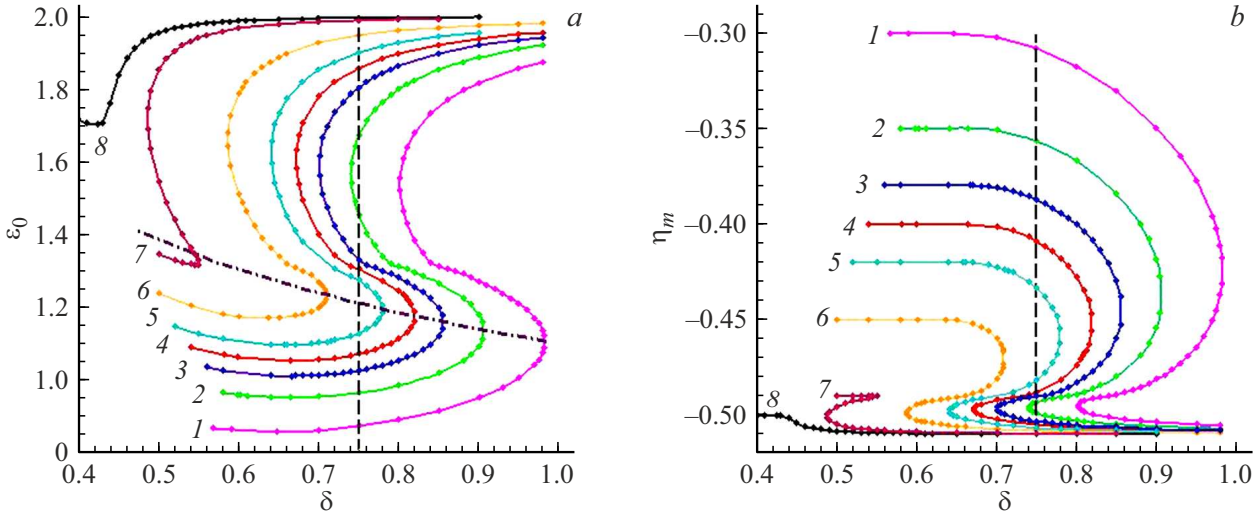

Figure 1. *a* — representation of steady-state solutions on the $\{\varepsilon_0, \delta\}$ plane; *b* — dependence of potential at the minimum η_m on δ for some values of V: −0.30 (*1*), −0.35 (*2*), −0.38 (*3*), −0.40 (*4*), −0.42 (*5*), −0.45 (*6*), −0.49 (*7*) and −0.50 (*8*); $\Delta = 0.01$. A dot-and-dash curve shows *SCL* bifurcation points calculated using equation (3).

1. With $|\Delta V| \ll 1$, the transient process flows smoothly, changing between the steady-state solutions lying between the branches with $V = V_0 - |\Delta V|$ and $V = V_0 + |\Delta V|$. In this case $\varepsilon(\tau, 0)$ oscillates at the external voltage frequency, varying within the $(\varepsilon_{0,\min}(V_0 + |\Delta V|, 0.75), \varepsilon_{0,\min}(V_0 - |\Delta V|, 0.75))$ interval. Process variation boundedness is provided by the fact that the chosen value of δ always stays to the left of $\delta_{SCL}(V_0 - |\Delta V|))$, so solutions actually follow the steady-state solutions corresponding to the normal branches.

2. In the case when $|\Delta V|$ grows to values where $\delta_{SCL}(V_0 - \Delta V)$ turns out to be lower than $\delta = 0.75$ (for example, curve *6* in Figure 1, *a*), as the collector potential $V(\tau)$ decreases from V_0, the process initially follows the steady-state solutions lying on the normal branches corresponding to $V(\tau) > V_0 - |\Delta V|$. However, at a time τ^*, the right-hand $\delta_{SCL}(V(\tau^*))$ bifurcation point coincides with $\delta = 0.75$, and will be positioned to the left of $\delta = 0.75$ at the next nearest $\tau = \tau^* + \Delta\tau$. At $\tau^* + \Delta\tau$ with $\delta = 0.75$, there are no solutions from the normal branches any longer, and the diode has only stable solutions from the upper branch corresponding to $V = V(\tau^* + \Delta\tau)$. Numerical solutions below show that a transient solution will change to a solution corresponding to the upper branch with $V(\tau) > V_0 - |\Delta V|$. Then, process can go differently depending on $|\Delta V|$. If $\delta_{DF}(V_0 + |\Delta V|) < 0.75$ (for example, curve *2* in Figure 1, *a*), a transient solution will oscillate between the steady-state solutions from the upper branches corresponding to V from the $(V_0 - |\Delta V|, V_0 + |\Delta V|)$ range.

3. If $\delta_{DF}(V_0 + |\Delta V|) > 0.75$ (for example, curve *1* in Figure 1, *a*), the transient process moving over a region corresponding to solutions from the upper branches can „fall“ from this region and get into a region corresponding to solutions from the normal branches. After this, the process will follow steady-state solutions from this region and then will jump into a region of solutions corresponding to the upper branches. Thus, a transient solution will oscillate with changes between regions corresponding to both upper and lower branches.

Variables defining the transient process scenario

Scenario	ΔV	ω
1	−0.02	2.5
2	−0.05	0.25
3	−0.1	0.25

Numerical values of the variables defining the process scenario that will be further used for calculations are listed in the table.

Let's consider each of the above-listed scenarios in more detail.

2.1. Scenario 1

In case of $|\Delta V| \ll 1$ for δ-shaped $f_0(u_0)$, the transient process can be calculated analytically. We will adhere to study [18]. Until there are reflected particles, plasma state can be described by continuity, electron motion and Poisson equations

$$\partial_\tau n + \partial_\xi (un) = 0,$$

$$\partial_\tau u + u\partial_\xi u = \partial_\xi \eta,$$

$$\partial_\xi^2 \eta = n. \qquad (5)$$

Since $|\Delta V|$ is small, then variations of all quantities will be little different from steady-state ones corresponding to the collector potential $V = V_0$. They are denoted by the same

letter, but with a tilde on top: $X(\tau,\xi) = X_0(\xi) + \tilde{X}(\tau,\xi)$. We linearize system (5) with respect to small disturbances:

$$\partial_\tau \tilde{n} + \partial_\xi (u_0 \tilde{n}) + \partial_\xi (\tilde{u}/u_0),$$

$$\partial_\tau \tilde{u} + \partial_\xi (u_0 \tilde{u}) = \partial_\xi \tilde{\eta},$$

$$\partial_\xi^2 \tilde{\eta} = \tilde{n}. \tag{6}$$

Boundary conditions

$$\tilde{n}(\tau,0) = \tilde{u}(\tau,0) = \tilde{\eta}(\tau,0) = 0,$$

$$\tilde{\eta}(\tau,\delta) = \Delta V \sin(\omega\tau). \tag{7}$$

Problem (6), (7) is solved using the Laplace transform. The images are marked with index p. After transition to a new independent variable q — electron transit time from the emitter to point ξ — we get the following system of equations for the images

$$(u_0 \tilde{n}_p)' + p u_0 \tilde{n}_p + (\tilde{u}/u_0)' = 0,$$

$$(u_0 \tilde{u}_p)' + p u_0 \tilde{u}_p = \tilde{\eta}_p',$$

$$(\tilde{\eta}_p'/u_0)' = u_0 \tilde{n}_p, \tag{8}$$

with boundary conditions

$$\tilde{n}_p(0) = \tilde{u}_p(0) = \tilde{\eta}_p(0) = 0,$$

$$\tilde{\eta}_p(\delta) = \Delta V[\omega/(p^2+\omega^2)]. \tag{9}$$

In (8), the prime denotes a derivative with respect to q. If $\tilde{n}_p$ and $\tilde{u}_p$ from the 2nd and 3rd equations are expressed in terms of $\tilde{\eta}_p$, substituted into equation (1) and integrated using the boundary conditions from (9), then system (8) can be reduced to a single integro-differential equation for $\tilde{\eta}_p'$

$$\left(\frac{1}{u_0}\tilde{\eta}_p'\right)' + \frac{p}{u_0}\tilde{\eta}_p' + \frac{1}{u_0^2} e^{-pq} \int_0^q dy\, e^{py}\, \tilde{\eta}_p'(y) = p\tilde{\eta}_p'(0). \tag{10}$$

For solution of equation (10), it is convenient to proceed to a new desired function

$$Q(q) = u_0(q) \int_0^q \frac{dx}{u_0^2(x)} \int_0^x dy\, e^{py}\, \tilde{\eta}_p'(y). \tag{11}$$

$\eta_p'(q)$ is expressed in terms of $Q(q)$:

$$\eta_p' = (u_0 Q'' - u_0'' Q)\, e^{-pq}. \tag{12}$$

As a result equation (10) is reduced to

$$Q''' + (1-u_0'')u_0^{-1} Q' - [(1-u_0'')u_0' + u_0 u_0''']u_0^{-2} Q = p\tilde{\eta}_p'(0) e^{pq} \tag{13}$$

with boundary conditions

$$Q(0) = Q'(0) = 0, \quad Q''(0) = \tilde{\eta}_p'(0). \tag{14}$$

In the Bursian diode, $u_0(q) = q^2/2 - \varepsilon_0 q + 1$, $u_0''(q) = 1$, $u_0'''(q) = 0$. After substituting these expressions into (13), only a term with Q''' remains in left-hand side of the equation. After integrating the derived equation and substituting the found function Q into (12), we find $\tilde{\eta}_p'$. After integrating it with respect to q and considering the first boundary condition at the emitter in (9), we get an expression for $\tilde{\eta}_p$:

$$\tilde{\eta}_p(\xi) = \frac{\tilde{\eta}_p'(0)}{p^3} h_p(\xi). \tag{15}$$

Here

$$h_p(\xi) = \left[p^3\xi - pq + 2 - (2+pq)\, e^{-pq}\right]. \tag{16}$$

After using the boundary condition at the collector (9), we derive a resultant expression for a potential disturbance image

$$\tilde{\eta}_p(\xi) = \Delta V \frac{\omega}{p^2+\omega^2} \frac{h_p(\xi)}{h_p(\delta)}. \tag{17}$$

We also write expressions for images of electric field strength disturbance at the emitter and electron concentration distribution disturbance

$$\tilde{\varepsilon}_p(0) = -\Delta V \frac{\omega}{p^2+\omega^2} \frac{p^3}{h_p(\delta)},$$

$$\tilde{n}_p(q) = \Delta V \frac{\omega}{p^2+\omega^2} \frac{p}{u_0^3(q) h_p(\delta)}$$

$$\times \left\{u_0'(q) - \left(q[pu_0'(q) + p^2 u_0(q)] + u_0'(q)\right)e^{-pq}\right\}. \tag{18}$$

Original functions shall be recovered by the inverse Laplace transform. It is defined by zeroes of the function

$$h_p(\delta) = \left[p^3\delta - pT + 2 - (2+pT)\, e^{-pT}\right], \tag{19}$$

where T is the time of electron transit through the interelectrode gap, and by another two poles

$$p_\pm = \pm i\,\omega. \tag{20}$$

It should be noted that, unlike [19], where point $p = 0$ is a pole, in this problem all three images in equations (17), (18) have no peculiar features at point $p = 0$.

First, we calculate the original of $\tilde{\varepsilon}(\tau, 0)$. We write an expression for $h_p(\delta)$ (19) as

$$h_p(\delta) = R(p) - S(p)\, \exp(-pT),$$

$$R(p) = p^3\delta - pT + 2, \quad S(p) = 2 + pT$$

and expand the first expression in (18) in power series of $\exp(-pT)$

$$\tilde{\varepsilon}_p(0) = -\Delta V \sum_0^\infty \frac{\omega p^3 S^k(p)}{(p^2+\omega^2) R^{k+1}(p)} \exp(-kpT)$$

$$= -\Delta V \sum_0^\infty \frac{Q_k(p)}{P_k(p)} \exp(-kpT). \tag{21}$$

Here, $Q_k(p) = \omega p^3 S^k(p)$, $P_k(p) = (p^2 + \omega^2) R^{k+1}(p)$. The polynomial $R(p)$ has three roots: one real root p_1 and two complex-conjugate roots $p_{2,3}$ [20]:

$$p_1 = -\Gamma, \quad p_{2,3} = \Gamma/2 \pm i\Omega. \tag{22}$$

Here, $\Gamma = \alpha x + x^{-1}$, $\Omega = \sqrt{3}/2(\alpha x - x^{-1})$, $\alpha = T/(3\delta)$, $x = \left[\delta/(1 - \sqrt{\delta^2/\alpha^3}\right]^{1/3}$. The polynomial $P_k(p)$ has another two roots $p_\pm = \pm\omega$.

Taking into account that the image of $F(p)\exp(-a\,p)$ has $f(t-a)\,\Theta(t-a)$ as its original, we get the following expression for original $\tilde{\varepsilon}_0(\tau, 0)$

$$\tilde{\varepsilon}(\tau, 0) = -\Delta V \sum_{k=1}^{N} f^k(\tau_k)\,\Theta(\tau_k). \tag{23}$$

Here, $\tau_k = \tau - (k-1)T$, $N = [\tau/T] + 1$, and $f^k(\tau)$ is the original of $Q_k(p)/P_k(p)$. According to [21], $f^k(\tau)$ can be written as

$$f^k(\tau) = \sum_{m=1}^{3} \sum_{l=1}^{k} \frac{\Psi_{klm}(p_m)}{(k-l)!(l-1)!}\,\tau^{k-1}\,e^{p_m\tau}$$

$$+\Psi_{kl}(p_+)\,e^{p_+\tau} + \Psi_{kl}(p_-)\,e^{p_-\tau}.$$

Here

$$\Psi_{klm}(p_m) = \frac{d^{l-1}}{dp^{l-1}}\left[\frac{Q_k(p)}{P_{km}(p)}\right], \quad P_{km}(p) = P_k(p)/(p-p_m)^k,$$

$$\Psi_k(p_+) = \frac{Q_k(p)}{P_{k_+}(p)}, \quad P_{k_+}(p) = P_k(p)/(p-p_+),$$

$$\Psi_k(p_-) = \frac{Q_k(p)}{P_{k_-}(p)}, \quad P_{k_-}(p) = P_k(p)/(p-p_-). \tag{24}$$

For a complex-conjugate pair of p_2 and p_3, a sum of corresponding summands can be rearranged to

$$\Psi_{kl2}(p_2)\,e^{p_2\tau} + \Psi_{kl3}(p_3)\,e^{p_3\tau} = 2\,e^{\Gamma/2\tau}$$

$$\times\left[Re\,\Psi_{kl2}(p_2)\cos(\Omega\tau) - Im\,\Psi_{kl2}(p_2)\sin(\Omega\tau)\right]. \tag{25}$$

Similarly, for a sum of summands with p_+, p_-, we have

$$\Psi_k(p_+)\,e^{p_+\tau} + \Psi_k(p_-)\,e^{p_-\tau}$$

$$= 2\left[Re\,\Psi_k(p_+)\cos(\omega\tau) - Im\,\Psi_k(p_+)\sin(\omega\tau)\right]. \tag{26}$$

Finally for $f^k(\tau)$ we get

$$f^k(\tau) = e^{-\Gamma\tau}\sum_{l=1}^{k}\frac{\Psi_{k1l}(p_1)}{(k-l)!(l-1)!}\,\tau^{k-1} + 2\,e^{(\Gamma/2)\tau}$$

$$\times\sum_{l=1}^{k}\frac{Re\,\Psi_{kl2}(p_2)\cos(\Omega\tau) - Im\,\Psi_{kl2}(p_2)\sin(\Omega\tau)}{(k-l)!(l-1)!}\,\tau^{k-1}$$

$$+2\left[Re\,\Psi_k(p_+)\cos(\omega\tau) - Im\Psi_k(p_+)\sin(\omega\tau)\right]. \tag{27}$$

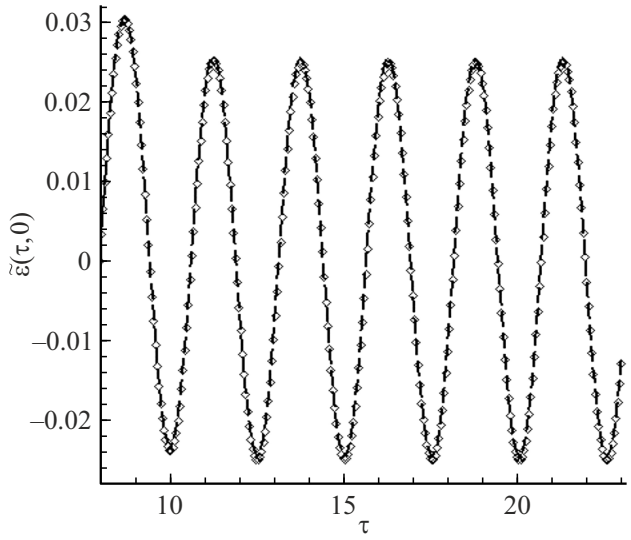

Figure 2. Evolution of electric field strength disturbance at the emitter $\tilde{\varepsilon}(\tau, 0)$ built using analytic equations (circles) and obtained in calculations with $\Delta = 0.01$ (dashed curves). $\delta = 0.75$, $V_0 = -0.40$, $\Delta V = -0.02$, $\omega = 2.5$.

Note that with $\tau \gg T$ it is difficult to use equation (23) for calculating the original, and the dependence of the original on time can be conveniently approximated by asymptotics of $\tilde{\varepsilon}(\tau, 0)$ at $\tau \to \infty$. It can be easily found by summing the residues $\tilde{\varepsilon}_p(0)\exp(p\tau)$ at poles p_+ and p_-, and is written as

$$\tilde{\varepsilon}(\tau, 0) \sim \frac{\Delta V\omega^3}{A^2 + B^2}\left(A\cdot\cos(\omega\tau) + B\cdot\sin(\omega\tau)\right),$$

$$A = 2 - 2\cos(\omega T) - \omega T\sin(\omega T),$$

$$B = -\omega^3\delta - \omega T + 2\sin(\omega T) - \omega T\cos(\omega T). \tag{28}$$

Equations (23)–(28) make it possible to build time variation of the electric field strength at the emitter $\varepsilon(\tau, 0) = \varepsilon_0 + \tilde{\varepsilon}(\tau, 0)$. Circles in Figure 2 show the evolution of field disturbance $\tilde{\varepsilon}(\tau, 0)$. As was predicted above, the field disturbance oscillates with the frequency ω. When looking at the strength $\varepsilon(\tau, 0)$ itself, adding the initial value $\varepsilon_0 = 1.071$ to the disturbance, it can be seen that it varies within the interval, whose boundaries correspond to the steady-state solution field strengths for the normal branch with $V = V_0 + 0.02$ ($\varepsilon_0 = 1.025$) and the normal branch with $V = V_0 - 0.02$ ($\varepsilon_0 = 1.128$). The $\varepsilon(\tau, 0)$ variation interval is equal to (1.047,1.096).

Now calculate the image of potential disturbance $\tilde{\eta}_p(\xi)$ (17), and then build the original of this function. By analogy with the foregoing, we convert (17), expanding this

expression in power series of $\exp(-pT)$:

$$\begin{aligned}\tilde{\eta}_p(\xi) =& \Delta V \frac{\omega}{p^2+\omega^2}\frac{h_p(\xi)}{h_p(\delta)}\\ =& \Delta V \frac{\omega}{p^2+\omega^2}\left[\frac{s(p,\xi)}{h_p(\delta)} - \frac{r(p,\xi)}{h_p(\delta)}e^{-pq}\right]\\ =& \Delta V\omega\left[\sum_{k=1}^{\infty}\frac{s(p,\xi)\,S(p)^{k-1}}{(p^2+\omega^2)\,R(p)^k}\,e^{-p(k-1)T}\right.\\ &\left.-\sum_{k=1}^{\infty}\frac{r(p,\xi)\,S(p)^{k-1}}{(p^2+\omega^2)\,R(p)^k}\,e^{-p[(k-1)T+q]}\right]\\ =& \Delta V\omega\left[\sum_{k=1}^{\infty}\frac{z_k(p,\xi)}{P_k(p)}\,e^{-p(k-1)T}\right.\\ &\left.-\sum_{k=1}^{\infty}\frac{w_k(p,\xi)}{P_k(p)}\,e^{-p[(k-1)T+q]}\right]. \end{aligned} \tag{29}$$

Here

$$\begin{gathered} s(p,\xi) = p^3\xi - pq + 1, \quad r(p,\xi) = pq + 2,\\ P_k(p) = (p^2+\omega^2)\,R^{k+1}(p),\\ z_k(p,\xi) = s(p,\xi)\,S^{k-1}(p), \;\; w_k(p,\xi) = r(p,\xi)\,S^{k-1}(p), \end{gathered} \tag{30}$$

and ξ is related to q through $\xi(q) = q^3/6 - \varepsilon_0 q^2/2 + q$. After performing the inverse Laplace transform for original, we get

$$\begin{aligned}\tilde{\eta}(\tau,\xi) =& \Delta V\omega\left[\sum_{k=1}^{m} g^{(k)}(\tau_k,\xi)\,\Theta(\tau_k)\right.\\ &\left.+\sum_{k=1}^{m} h^{(k)}(\tau_k - q,\xi)\,\Theta(\tau_k - q)\right]. \end{aligned} \tag{31}$$

Here, $\tau_k = \tau - (k-1)T$, $N = [\tau/T] + 1$, and $g^{(k)}(\tau,\xi)$ and $h^{(k)}(\tau,\xi)$ are the originals of $z_k(p,\xi)/P_k(p)$ and $w_k(p,\xi)/P_k(p)$, respectively. $g^{(k)}(\tau,\xi)$ can be written as

$$\begin{aligned} g^{(k)}(\tau,\xi) =& \sum_{m=1}^{3}\sum_{l=1}^{k}\frac{G_{klm}(\xi,p_m)}{(k-l)!(l-1)!}\,\tau^{k-1}\,e^{p_m\tau}\\ &+G_k^+(\xi,p_+)\,e^{p_+\tau} + G_k^-(\xi,p_-)\,e^{p_-\tau}. \end{aligned}$$

Here

$$\begin{gathered} G_{klm}(\xi,p) = \frac{d^{l-1}}{dp^{l-1}}\left[\frac{z_k(\xi,p)}{P_{km}(p)}\right],\\ G_k^+(\xi,p) = \frac{z_k(\xi,p)}{P_{k_+}(p)},\\ G_k^-(\xi,p) = \frac{z_k(\xi,p)}{P_{k_-}(p)}. \end{gathered} \tag{32}$$

By grouping coefficients of the complex-conjugate roots, equation (32) can be rewritten as

$$\begin{aligned} g^{(k)}(\tau,\xi) =& e^{-\Gamma\tau}\sum_{l=1}^{k}\frac{G_{kl1}(\xi,p_1)}{(k-l)!(l-1)!}\,\tau^{k-1}2\,e^{(\Gamma/2)\tau}\\ &\times\sum_{l=1}^{k}\frac{Re\,G_{kl2}(\xi,p_2)\cos(\Omega\tau) - Im\,G_{kl2}(\xi,p_2)\sin(\Omega\tau)}{(k-l)!(l-1)!}\tau^{k-1}\\ &+2\left[Re\,G_k^+(\xi,p_+)\cos(\omega\tau) - Im\,G_k^+(\xi,p_+)\sin(\omega\tau)\right]. \end{aligned} \tag{33}$$

Similarly, we get an expression for $h^{(k)}(\tau,\xi)$:

$$\begin{aligned} h^{(k)}(\tau,\xi) =& e^{-\Gamma\tau}\sum_{l=1}^{k}\frac{H_{kl1}(\xi,p_1)}{(k-l)!(l-1)!}\,\tau^{k-1} + 2\,e^{(\Gamma/2)\tau}\\ &\times\sum_{l=1}^{k}\frac{Re\,H_{kl2}(\xi,p_2)\cos(\Omega\tau) - Im\,H_{kl2}(\xi,p_2)\sin(\Omega\tau)}{(k-l)!(l-1)!}\tau^{k-1}\\ &+2\left[Re\,H_k^+(\xi,p_+)\cos(\omega\tau) - Im\,H_k^+(\xi,p_+)\sin(\omega\tau)\right]. \end{aligned} \tag{34}$$

Here

$$\begin{gathered} H_{klm}(\xi,p) = \frac{d^{l-1}}{dp^{l-1}}\left[\frac{w_k(\xi,p)}{P_{km}(p)}\right],\\ H_k^+(\xi,p) = \frac{w_k(\xi,p)}{P_{k_+}(p)},\\ H_k^-(\xi,p) = \frac{w_k(\xi,p)}{P_{k_-}(p)}. \end{gathered} \tag{35}$$

As in calculation of $\tilde{\varepsilon}(\tau,0)$, for $\tau >> T$, it is convenient to use, instead of these equations, the asymptotics of $\tilde{\eta}(\tau,\xi)$ at $\tau\to\infty$, which is written as

$$\begin{aligned}\tilde{\eta}(\tau,\xi) \sim& \frac{-\Delta V}{A^2+B^2}\left[(A\omega^3\xi - A\omega q - 2B)\cdot\cos(\omega\tau)\right.\\ &+(B\omega^3\xi - B\omega q + 2A)\cdot\sin(\omega\tau)\\ &+(2B - A\omega q)\cdot\cos(\omega(\tau - q))\\ &\left.-(2A + B\omega q)\cdot\sin(\omega(\tau - q))\right]. \end{aligned} \tag{36}$$

Here, constants A and B are calculated using equations (28), and $\xi = q^3/6 - (\varepsilon_0/2)q^2 + q$.

Calculations performed using equations (31)–(36) show that time distributions of potential disturbance over the gap $\tilde{\eta}(\tau,\xi)$ vary periodically with the period $T_\omega = 2\pi/\omega$. Such distributions for a set of times within an oscillation period are shown in Figure 3.

This process was also numerically calculated using a high-precision E,K-code. The underlying algorithm of the code is described in detail, for example, in [16]. In calculations, the electron velocity distribution function was chosen in the form of an arch (2) with $\Delta = 0.01$. The presence of a small velocity spread for the electron distribution

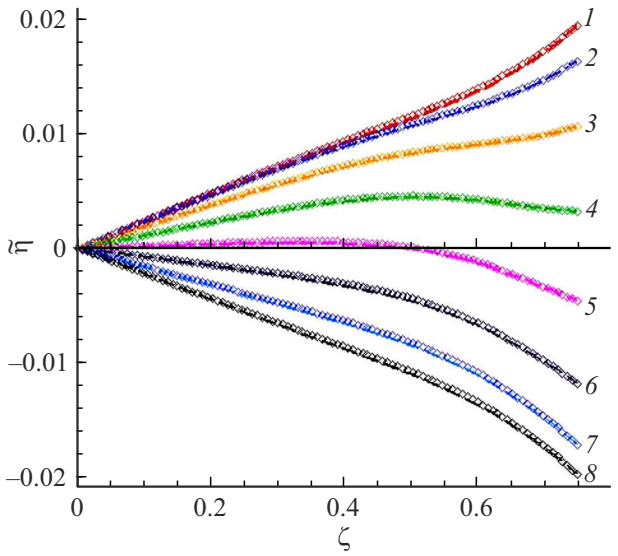

Figure 3. Dependences of the PD disturbance $\tilde{\eta}(\tau, \xi)$ within an oscillation period for a set of times τ: 20.02 (*1*), 20.18 (*2*), 20.34 (*3*), 20.50 (*4*), 20.66 (*5*), 20.82 (*6*), 20.98 (*7*), 21.14 (*8*). Curves marked with circles were calculated using analytical equations, dashed curves are the results of calculations with $\Delta = 0.01$. $\delta = 0.75$, $V_0 = -0.40$, $\Delta V = -0.02$, $\omega = 2.5$.

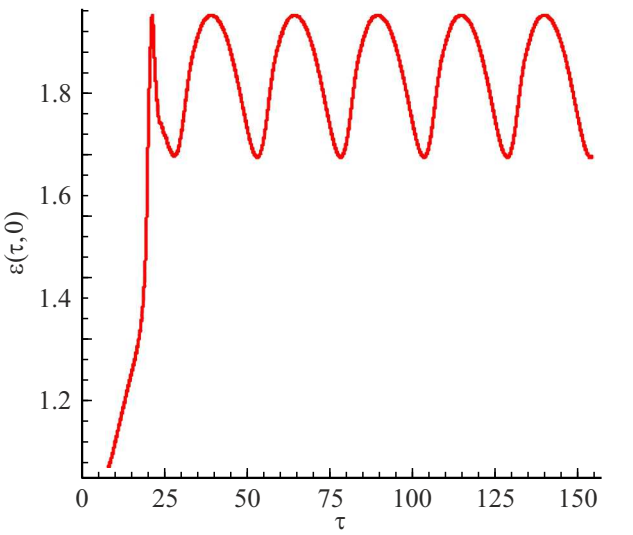

Figure 4. Time dependence of the electric field strength at the emitter; $\delta = 0.75$, $V_0 = -0.40$, $\Delta V = -0.05$, $\omega = 0.25$. $\Delta = 0.01$.

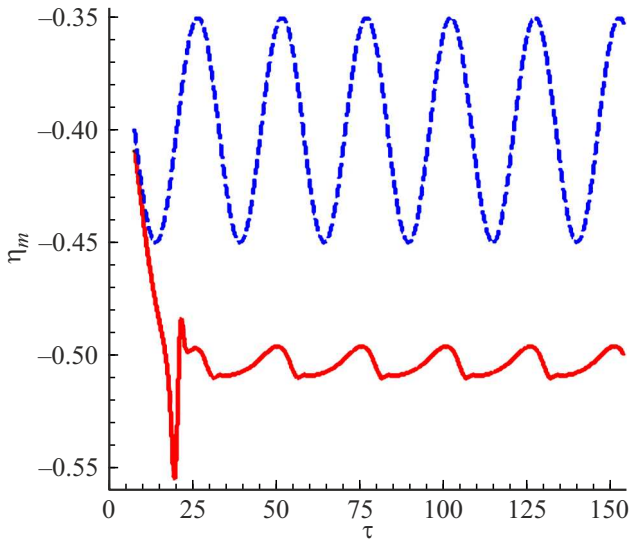

Figure 5. Time dependence of the potential at the minimum (solid curve). Dashed curve shows the time variation of the collector potential. $\delta = 0.75$, $V_0 = -0.40$, $\Delta V = -0.05$, $\omega = 0.25$. $\Delta = 0.01$.

function shall not affect heavily the process flow. The following variables were chosen for calculation: $\tau_0 = 8.0$, $\Delta V = -0.02$, $\omega = 2.5$ ($T_\omega \approx 2.5$). For the gap, 200 point of division were used, and count step $\Delta\tau = 0.02$.

After a short transient process, periodic oscillations were established in the diode. Figure 2 demonstrates the evolution of the electric field strength disturbance at the emitter, and Figure 3 shows PD disturbances for a set of times within an oscillation period Numerical calculation results are shown by dashed curves, and dependences found using analytical equations are shown by circles. Good coincidence of numerical and analytical results can be seen.

Plasma state evolution was calculated for the same $\Delta V = -0.02$, but with a lower external frequency $\omega = 0.25$. The process also achieved oscillations, with their amplitude being the same as that with the above-mentioned variables, but they has a larger period $T_\omega = 2\pi/\omega \approx 25$.

2.2. Scenario 2

The same diode variables as in Section 2.1 were chosen for calculation: $\delta = 0.75$, $V = V_0 = -0.40$, but the collector potential oscillation amplitude was increased: $\Delta V = -0.05$ and the external frequency was decreased: $\omega = 0.25$. Figure 4 shows the evolution of the electric field strength at the emitter $\varepsilon(\tau, 0)$. It can be seen that a mode with oscillations with the period $T_\omega = 2\pi/\omega \approx 25$ is set after a quite sudden transient process. Transient solution initially follows the states located in the neighborhood of the normal branches as in Scenario 1, but then it changes to a solution located in the neighborhood of the upper branches. As mentioned above, corresponding steady-state solutions are stable. But as $\delta_{BF}(V_0 + 0.05)$ and, especially, $\delta_{BF}(V_0 - 0.05)$ turn out to be lower than $\delta = 0.75$, then the nonsteady process cannot „leave“ the neighborhood of these solutions to solutions on the normal branch. As a result, it remains in the neighborhood of solutions on the upper branches where it oscillates, while the oscillation amplitude $\varepsilon(\tau, 0)$ turns out to be relatively small — field strengths at the emitter $\varepsilon(\tau, 0)$ vary within $(1.674, 1.950)$. As can be seen from Figure 1, *a*, field strengths at the emitter ε_0 at $\delta = 0.75$ for extreme steady-state solutions corresponding

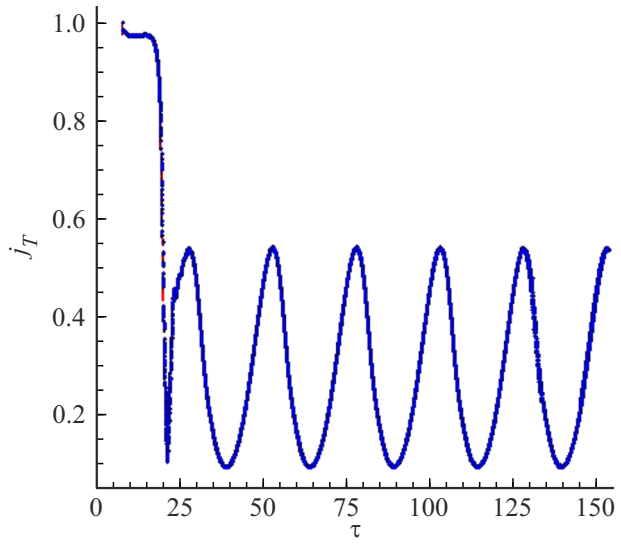

Figure 6. Time dependences of the total current at the emitter (dashed curve) and collector (circles); $\delta = 0.75$, $V_0 = -0.40$, $\Delta V = -0.05$, $\omega = 0.25$. $\Delta = 0.01$.

to $V = -0.35$ and -0.45 are within $(1.675, 1.949)$. Thus, transient plasma characteristics don't leave the region of existence of steady-state solutions corresponding to the upper branch

Figure 5 shows the evolution of the potential at the VC vertex η_m. It can be seen that after a quite sudden transient process, η_m achieves the steady-state oscillations. The oscillations are nonlinear, but their amplitude turns out to be much smaller than $|\Delta V|$ — values of η_m vary in the range approximately from -0.51 to -0.495.

For verification of calculations, total currents at the emitter and collector were built (Figure 6). It can be seen that these currents coincide with a high level of accuracy. This confirms the known results: total current in plasma in a one-dimensional diode doesn't depend on a coordinate.

2.3. Scenario 3

The same diode variables as in Section 2.2 were chosen for calculation, but the collector potential oscillation amplitude was increased: $\Delta V = -0.10$. Figure 7 shows the evolution of the electric field strength at the emitter. It can be seen that the solution quite suddenly changes from the region of steady-state solutions located in the neighborhood of the normal branches (Figure 1, *a*) to the neighborhood of solutions corresponding to the upper branches.

As in Scenario 2, this is due to the fact that when $\delta_{SCL}(V(\tau))$ turn out to be lower than 0.75, there are no steady-state solutions corresponding to the normal branch, and there are only stable solutions from the upper branch that correspond to the collector potential at this point in time. However, unlike Scenario 2, here $\delta_{BF}(V_0 + 0.10)$ turns out to be higher than 0.75. Therefore, $\delta_{BF}(V(\tau))$ becomes equal to 0.75 at some time, and there are no solution in the upper branch region at the next nearest time. In this situation, the solution is able to get back to the neighborhood of states corresponding to the normal branches, and this is the case. Then the solution again gets into the neighborhood of steady-state solutions corresponding to the upper branches, etc. As a result, a mode with strictly periodic oscillations with $T_\omega = 2\pi/\omega \approx 25$ is established in the diode.

Unlike Scenario 2, where the transient solution remains in the neighborhood of steady-state solutions corresponding to the upper branches, here oscillations have a complex structure, and the electric field strength oscillation amplitude at the emitter turns out to be quite large (varies within $(0.904, 2.234)$. For steady-state solutions corresponding to extreme collector potentials: $V = -0.3$ and -0.5, the ε_0 variation interval is equal to $(0.872, 1.987)$. Thus, it can be seen that, when the collector potential of the transient solution corresponds to steady-state solutions within the normal branch region (Figure 8), the electric field strengths at the emitter don't go beyond the lower boundary of the region of existence of steady-state solutions. When $\eta(\tau, \delta)$ gets into a region of steady-state solutions corresponding to the upper branches, the neighborhood of the $\varepsilon(\tau, 0)$ maximum during a small part of the oscillation period can go beyond the region of values corresponding to steady-state solutions with $V = V_0 - 0.1 = -0.5$.

Figure 8 shows the oscillations of the VC vertex potential $\eta_m(\tau)$. It can be seen that oscillations of η_m are synchronous with the collector potential oscillations. It can be also seen that η_m during a small part of the oscillation period is lower than the collector potentials existing at these times. Then the values of $\varepsilon(\tau, 0)$ go beyond the boundaries of the region corresponding to steady-state solutions with these $V(\tau)$.

We enlarge on the characteristics of a solution within an oscillation period. Figure 9 – 11 shows time variations of the potential at the minimum, coordinates of the potential,

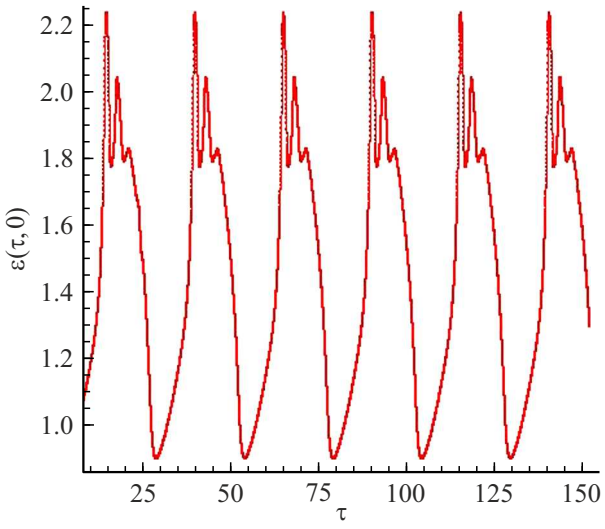

Figure 7. Time dependence of the electric field strength at the emitter; $\delta = 0.75$, $V_0 = -0.40$, $\Delta V = -0.10$, $\omega = 0.25$. $\Delta = 0.01$.

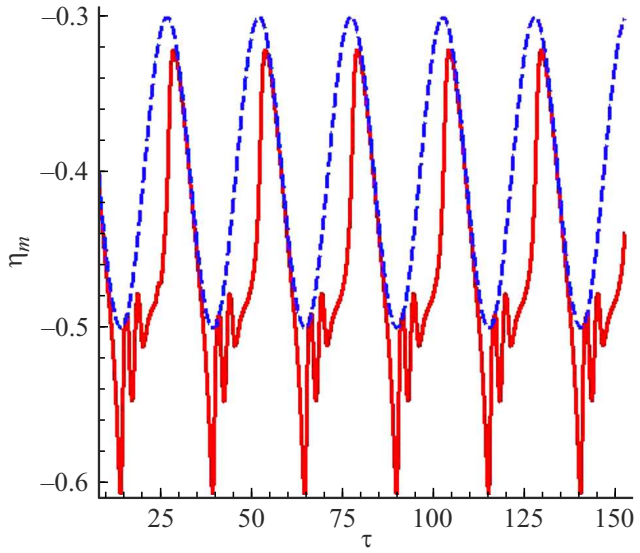

Figure 8. Time dependences of the potential at the minimum η_m (solid curve). Dashed curve shows the time variation of the collector potential. $\delta = 0.75$, $V_0 = -0.40$, $\Delta V = -0.10$, $\omega = 0.25$. $\Delta = 0.01$.

electric field strengths, and convection currents at the emitter and collector. It can be seen that, unlike Scenario 2 (Figures 4 and 5), change of the transient solution to the upper branch region is followed by oscillations with a higher frequency. Figure 9 shows that during a period of time η_m becomes lower than $V_0 - |\Delta V|$ or even occurs at the collector, i.e. PD becomes monotonic. During these periods of time, very few electrons reach the collector surface (Figure 10, *b*). Figure 10, *a* shows that the convection current at the emitter remains equal to the emission current during almost a half of the oscillation period. This suggests that reflected electrons don't reach the emitter within this period of time. It can be also seen that the reflected electron flux during some periods of time exceeds the direct particle flux ($j_E < 0$). Figure 10, *b* shows that very few electrons reach the collector at certain periods of time, but many electrons are „discharged" at the collector at some points in time.

The electric field strengths at the emitter and collector also have a sufficiently complex structure where solutions occur in the neighborhood of steady-state solutions from the upper branches (Figure 11). At times when η_m is lower than $V_0 - |\Delta V|$, solutions can even go beyond the region corresponding to the steady-state solutions of branches with reflection.

Figure 12 shows the evolution of total currents at the emitter and collector during the oscillation period. It can be seen that the currents coincide with a high level of accuracy. This proves that the calculations are correct.

Conclusion

During investigation of processes taking place in the Bursian diode in the presence of reactive elements of an external circuit, it shall be understood what steady-state solutions can be implemented in the diode plasma when the external voltage is not constant, but varies with time. The study has identified and examined the main types of transient solutions that can be implemented in the Bursian diode plasma for the case of a predefined external harmonic time-varying voltage. It is shown that solutions have a form of an oscillatory process with a frequency equal to an external voltage oscillation frequency. It has been found that the progress of the transient process is to a great extent defined by the regions of „attraction" of steady-state solutions at the diode with collector potentials falling within the external voltage variation region — $(V_0 - |\Delta V|, V_0 + |\Delta V|)$.

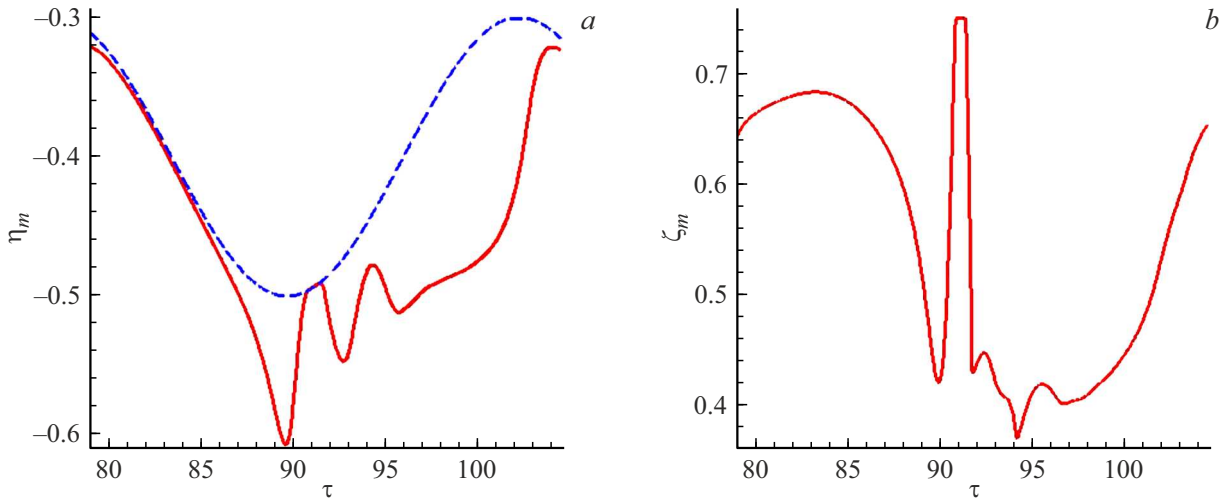

Figure 9. Variation (*a*) of potential at the minimum η_m and (*b*) position of the potential ξ_m during the oscillation period. Dashed curve shows how the collector potential varies. $\delta = 0.75$, $V_0 = -0.40$, $\Delta V = -0.10$, $\omega = 0.25$. $\Delta = 0.01$.

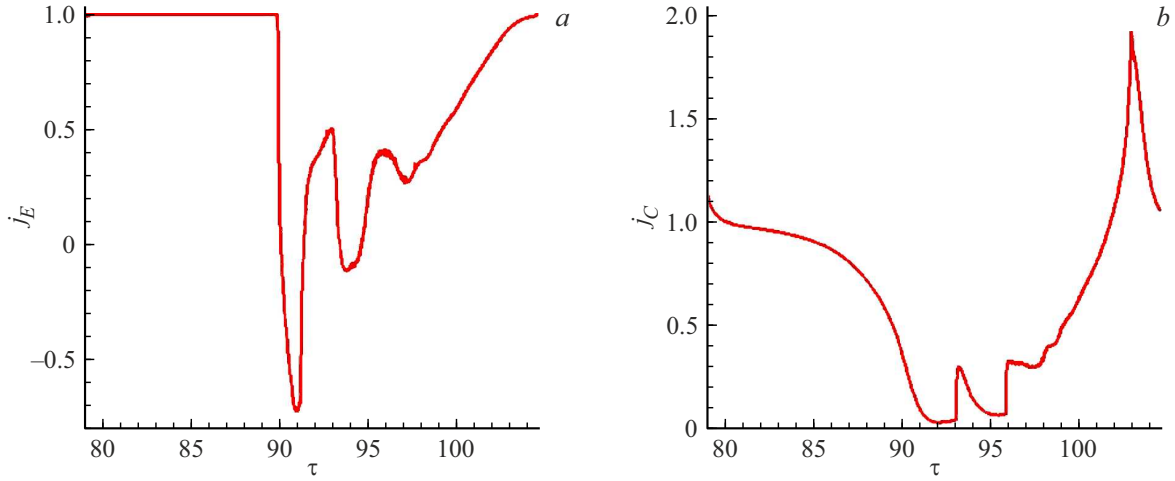

Figure 10. Evolution of the (a) convection current at the emitter j_E and (b) at the collector j_C during the oscillation period; $\delta = 0.75$, $V_0 = -0.40$, $\Delta V = -0.10$, $\omega = 0.25$. $\Delta = 0.01$.

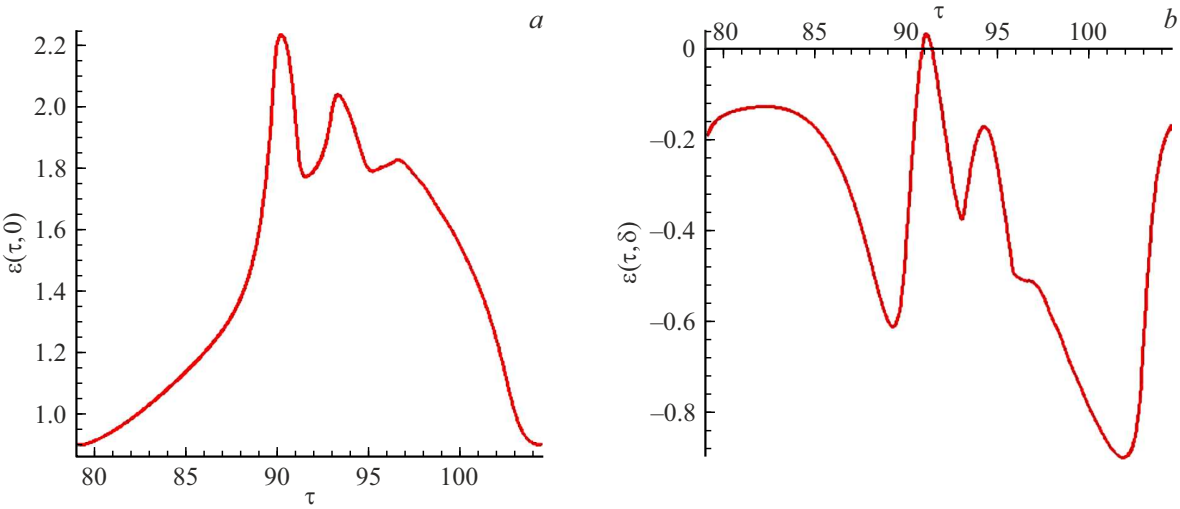

Figure 11. Evolution of the electric field strength at the (a) emitter $\varepsilon(\tau, 0)$ and (b) collector $\varepsilon(\tau, \delta)$ during the oscillation period; $\delta = 0.75$, $V_0 = -0.40$, $\Delta V = -0.10$, $\omega = 0.25$. $\Delta = 0.01$.

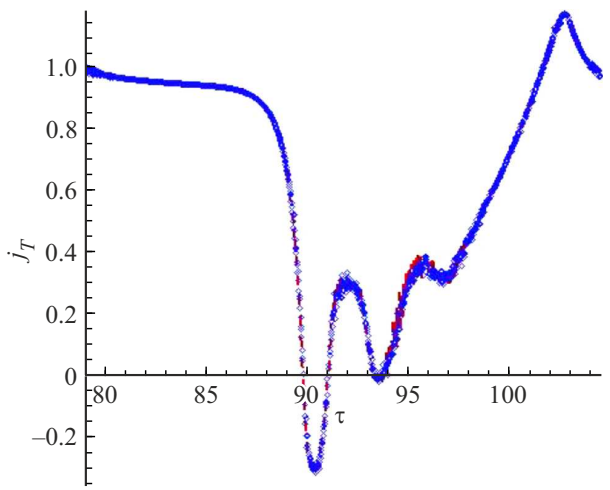

Figure 12. Time dependence of the total current at the emitter (dashed curve) and collector (circles) during the oscillation period; $\delta = 0.75$, $V_0 = -0.40$, $\Delta V = -0.10$, $\omega = 0.25$. $\Delta = 0.01$.

Three types of transient solutions have been found by means of the analysis of steady-state solutions at the diode with various constant external voltages from the specified region, and of the results of numerical calculations of transient processes in the diode plasma, to which an alternating external voltage was applied. At small external voltage oscillation amplitudes ($|\Delta V| \ll 1$), the electric field in plasma oscillates with an amplitude on the order of $|\Delta V|$. In this case, the transient solutions actually „follows“ the steady-state solutions corresponding to the normal branches with collector potentials running through the $(V_0 - |\Delta V|, V_0 + |\Delta V|)$ region. An analytical solution has been obtained for this case. Results of process calculations using the E,K-code coincided with this analytical solution with a high level of accuracy.

As the amplitude $|\Delta V|$ increases to the values where the interelectrode gap δ turns out to be greater than $\delta_{SCL}(V_0 - |\Delta V|)$, an opportunity of implementing another two types of transient solutions arises. In the case when

$\delta > \delta_{BF}(V_0 + |\Delta V|)$, transient solutions always oscillate in the neighborhood of steady-state solutions corresponding to the upper branches with electron reflection.

In the case when $\delta < \delta_{BF}(V_0 + |\Delta V|)$, transient solutions are also periodic, but are in the neighborhood of solutions corresponding to the branches with reflection only during a part of the period. Then they are able to jump into the neighborhood of solutions from the lower branches where they spend the remaining part of the period. Then the transient solutions return again into the neighborhood of the upper branches and the process is repeated.

The work is a continuation of paper [17]. Both papers discuss two fundamentally different methods of transition between stable the Bursian diode states: spontaneous transition caused by internal plasma instability and controlled transition caused by an external sinusoidal impact. In [17], it is explained why the system in general can change its states, and „natural" ways of system evolution are also demonstrated. It is shown how an alternating external voltage can be used for targeted control of system states, inducing complex nonlinear oscillations and jumping. As a result, a complete picture of transient behavior of a complex nonlinear system such as the Bursian diode has been built. The findings can be used as the basis for design of devices utilizing such diode.

The study provides the tools for analysis of processes in the diode — external circuit system in the presence of reactive circuit elements and as well as in TIC operating in AC generation mode. Thus, the work not only contributes to the fundamental physics of nonlinear oscillations in plasma diodes, but also provides a particular mechanism of active system state control, opening the way to the development of a new generation of TIC that can effectively generate alternating current.

Acknowledgments

Sections 1.2 and 1.3 were completed with the financial support of the Russian Science Foundation, project №24-22-00175; Introduction and Section 1.1 were completed under a state order, Topic No. FFUG-2024-0005.

Conflict of interest

The authors declare no conflict of interest.

References

[1] K.A.A. Khalid, T.J. Leong, K. Mohamed. IEEE Transactions on Electron Devices, **63** (6), 2231 (2016). DOI: 10.1109/TED.2016.2556751

[2] D.B. Go, J.R. Haase, J. George, J. Mannhart, R. Wanke, A. Nojeh, R. Nemanich. Frontiers in Mechanical Engineering, **3** (13) (2017). DOI: 10.3389/fmech.2017.00013

[3] G. Xiaoa, G. Zhenga, M. Qiub, Q. Lib, D. Lic, M. Ni. Appl. Energy, **208**, 1318 (2017). DOI: 10.1016/j.apenergy.2017.09.021

[4] M.F. Campbell, T.J. Celenza, F. Schmitt, J.W. Schwede, I. Bargatin. Adv. Sci., **8**, 2003812 (2021). DOI: 10.1002/advs.202003812

[5] V.I. Babanin, A.Ya. Ender, I.N. Kolyshkin, V.I. Kuznetsov, V.I. Sitnov, D.V. Paramonov. Proc. 32nd IECEC (Honolulu, USA. AIChE, 1997), 427.

[6] V.I. Kuznetsov, A.Ya. Ender. ZhTF, **53** (12), 2329 (1983) (in Russian) Russian).

[7] V.I. Kuznetsov, A.B. Gerasimenko. J. Appl. Phys., **125**, 183301 (2019). DOI: 10.1063/1.5090204

[8] V.I. Kuznetsov, A.B. Gerasimenko, M.A. Zakharov. Plasma Phys. Rep., **51** (2), 155 (2025). DOI: 10.1134/S1063780X24601925

[9] A.E. Dubinov, V.D. Selemir. Radiotekhnika i elektronika, **47** (6), 645 (2002) (in Russian).

[10] S. Mumtaz, H.S. Uhma, E.H. Choi. Phys. Reports, **1069**, 1 (2024).

[11] A.E. Dubinov, V.D. Selemir. Radiotekhnika i elektronika, **49** (10), 1264 (2004) (in Russian).

[12] N.S.Frolov Izv. vuzov, PND, **20** (3), 152 (2012).(in Russian)

[13] A.A.Badarin, S.A.Kurkin, N.S.Frolov, A.O.Selsky, A.E.khramov, A.A.Koronovsky. Izv. RAN. Ser. Fizicheskaya, **78**, 11 (2014). (in Russian). DOI: 10.1134/S0367676518110042

[14] M. Siman-Tov, J.G. Leopold, Ya.E. Krasik. Phys. Plasma, **26**, 033113 (2019). DOI: 10.1063/1.5087708

[15] C.E. Fay, A.L. Samuel, W. Shockly. Bell Syst. Tech. J., **17**, 49 (1938).

[16] V.I. Kuznetsov, A.Ya. Ender. Fizika Plazmy, **36** (3), 248 (2010) (in Russian).

[17] V.I.Kuznetsov, V.Yu.Koyokin, M.A.Zakharov, I.K.Morozov. ZhTF, **94** (11), 1809 (2024) (in Russian) Russian). DOI: 10.61011/JTF.2024.11.59097.239-24

[18] P.V. Akimov, A.Ya. Ender, V.I. Kuznetsov, H. Schamel. J. Appl. Phys., **93** (2), 1246 (2003).

[19] N.M. Kuznetsov. Dokt.diss., (SPb, FTI im. Ioffe, 2006) (in Russian)

[20] G. Korn, T. Korn. *Spravochnik po matematike. Dlya nauchnyh rabotnikov*, (Nauka, M., 1974) (in Russian).

[21] G. Bateman, A. Erdane. *Tablitsy integral'nykh preobrazovaniy, t.1. Fur'ye, Laplasa, Mellina, tom 1969* (Nauka, M., 1969) (in Russian).

Translated by E.Ilyinskaya